Metabolomic analysis based on ^{1}H-nuclear magnetic resonance spectroscopy metabolic profiles in tuberculous, malignant and transudative pleural effusion

CHENG WANG, JINGJIN PENG, YANLING KUANG, JIAQIANG ZHANG and LUMING DAI

The Second Department of Respiratory Medicine,
The First Affiliated Hospital of Kunming Medical University, Kunming, Yunnan 650032, P.R. China

Received May 29, 2016; Accepted April 12, 2017

DOI: 10.3892/mmr.2017.6758

Abstract. Pleural effusion is a common clinical manifestation with various causes. Current diagnostic and therapeutic methods have exhibited numerous limitations. By involving the analysis of dynamic changes in low molecular weight catabolites, metabolomics has been widely applied in various types of disease and have provided platforms to distinguish many novel biomarkers. However, to the best of our knowledge, there are few studies regarding the metabolic profiling for pleural effusion. In the current study, 58 pleural effusion samples were collected, among which 20 were malignant pleural effusions, 20 were tuberculous pleural effusions and 18 were transudative pleural effusions. The small molecule metabolite spectrums were obtained by adopting ^{1}H nuclear magnetic resonance technology, and pattern-recognition multi-variable statistical analysis was used to screen out different metabolites. One-way analysis of variance, and Student-Newman-Keuls and the Kruskal-Wallis test were adopted for statistical analysis. Over 400 metabolites were identified in the untargeted metabolomic analysis and 26 metabolites were identified as significantly different among tuberculous, malignant and transudative pleural effusions. These metabolites were predominantly involved in the metabolic pathways of amino acids metabolism, glycometabolism and lipid metabolism. Statistical analysis revealed that eight metabolites contributed to the distinction between the three groups: Tuberculous, malignant and transudative pleural effusion. In the current study, the feasibility of identifying small molecule biochemical profiles in different types of pleural effusion were investigated reveal novel biological insights into the underlying mechanisms. The results provide specific insights into the biology of tubercular, malignant and transudative pleural effusion and may offer novel strategies for the diagnosis and therapy of associated diseases, including tuberculosis, advanced lung cancer and congestive heart failure.

Correspondence to: Professor Luming Dai, The Second Department of Respiratory Medicine, The First Affiliated Hospital of Kunming Medical University, 295 Xichang Road, Kunming, Yunnan 650032, P.R. China
E-mail: dailuming6622@hotmail.com

Key words: pleural effusion, metabolomic, ^{1}H-nuclear magnetic resonance technology, partial least squares discriminant analysis, one-way analysis of variance, Student-Newman-Keuls, Kruskal-Wallis test

Introduction

Pleural effusion is a common clinical manifestation worldwide, with an annual morbidity >3,000 per million people (1). The causes of pleural effusion are diverse. According to specific gravity, protein content and cell number of pleural effusion, and Light's criteria (2), pleural effusion is divided into transudative or exudative pleural effusion. In the clinical setting, transudative pleural effusion is usually caused by cardiac insufficiency, hypoproteinemia and hepatocirrhosis. Exudative pleural effusion is usually due to tuberculosis (TB) and tumors (3). The World Health Organization released a global TB report in 2015 (4); this report noted that in 2014, ~9.6 million individuals were infected with TB and 1.5 individuals succumbed. In recent years, the incidence of lung and pleural tumors is increasing. The mortality rate has been ranked first of the malignant tumors. Therefore, establishing a strategy to rapidly and accurately diagnose and determine the etiologies of pleural effusion patients is an issue that is difficult to solve. The current diagnostic methods have various limitations. The biopsy examination is traumatic and the compliance rate for patients is usually low. Furthermore, the cytology and pathogenic examinations often exhibit low sensitivity. With the development of laboratory techniques, enzymology and tumor marker examinations have been widely adopted in the clinical setting. Although adenosine deaminase, lactate dehydrogenase (LDH), carcinoembryonic antigen, CA 125, CA 199, cytokerantin-19-fragment (CYFRA 21-1) and neuron-specific enolase levels have been used to determine the diagnosis of pleural effusion type to a certain extent, they are considered to be of limited value. There continues to be numerous pleural effusion patients that have failed to receive rapid and accurate diagnoses and treatment (5). Data from a mathematical modeling study estimated that only 35% of pediatric cases of

TB were detected in 15 countries reporting pediatric and adult notifications by age in 2010 (6). Therefore, rapid and accurate diagnostic methods are urgently required.

Since the concept of metabonomics was put forward by Nicholson in 1999 (7), it has been developed rapidly and is widely used in clinical research. The metabolomic research methods (analyzing metabolic phenotype and metabolic dynamic changes of the body under different conditions) provide an improved understanding of the development process of disease, as well as the metabolic pathways and mechanisms of the inner body. This provides critical clues for diagnosis and treatment of disease, which is significant, not only in basic theory research, but in clinical application. As the ultimate downstream pool of genome transcription, metabolomics reflects what actually occurs in the living cells or organism, whereas genetics and proteomics only indicates what may have occurred (8,9). Evaluation of the dynamic changes in low molecular weight catabolites has been widely applied in various types of disease and provides a platform to distinguish novel biomarkers, for example in cancer (10,11), diabetes (12-14), hypertension (15), coronary heart disease (16-18), polycystic ovary syndrome (19), and major depressive disorder (20). However, there are few studies regarding the metabolic profiling for pleural effusion.

Applied to biomedical research at the beginning of the 1970s, ^{1}H nuclear magnetic resonance (^{1}H-NMR) spectroscopy, in which the relevant information was obtained by using an external magnetic field to change the energy of the atomic nucleus, was one of the earliest technologies applied for the analysis of metabolomics. There are various types of NMR techniques, such as ^{1}H-NMR, ^{13}C-NMR and ^{31}P-NMR. However, the most widely adopted is ^{1}H-NMR. NMR technology detects all of the metabolites in the sample and reflects the content of each metabolite through relative strength of the signal in a spectrum.

In the current study, NMR-based metabolomic technology was used to screen characteristic metabolic substances of patients with tuberculous, malignant or transudative pleural effusion, which are hypothesized to be potential markers of the disease state, in order to facilitate further clinical research. A partial least squares discriminant analysis (PLS-DA) model was established whilst constructing the metabolite profiles. A total of 58 patients, including 20 with tuberculous pleural effusion, 20 with malignant pleural effusion, and 18 with transudative pleural effusion were enrolled. Multivariate statistical analysis was implemented to distinguish between the three groups of patients on the basis of their metabolic profiles. Novel data processing and analysis techniques for metabolomics may provide a broader range of applications in disease diagnosis and classification. Furthermore, an in-depth knowledge of the metabolic profiling of pleural effusion may improve the understanding of the underlying mechanism of pulmonary TB, malignant and transudative pleural effusion, and reveal novel diagnostic and therapeutic methods for these diseases.

Materials and methods

Subjects. All participants were recruited from the Second Department of Respiratory Medicine in the First Affiliated Hospital of Kunming Medical University (Kunming, China) between August 2014 and September 2015. The study was approved by the ethics committee of Kunming Medical University and all aspects of the study were performed within the constraints laid out by the ethics committee. All patients involved in the study provided written informed consent.

The T group was formed of tuberculous pleural effusion patients (n=20), who were diagnosed following chest pain, dyspnea and other pleural effusion symptoms. In addition, patients exhibited afternoon fever, night sweats, fatigue, weight loss and other symptoms of TB. Upon chest physical examination, weakened tactile fremitus and percussion dullness were observed in the affected side, lung auscultation revealed weakened or disappeared breath sounds and chest CT examinations revealed pleural effusion, with or without pulmonary TB lesions. Routine examination of pleural fluid was performed according to Light's criteria to determine the exudate. Mycobacterium was detected as positive by pleural biopsy or airway secretion pathogen examination. In addition, treatment with anti-TB medication resulted in clinical and radiological improvement. Patients with metabolic diseases were excluded. Pleural effusion was collected from each participant prior to treatment with anti-TB medication.

The C group was formed of malignant pleural effusion patients (n=20), who were diagnosed following chest pain, dyspnea and other pleural effusion symptoms. Chest physical examination indicated weakened tactile fremitus and percussion dullness in the affected side. In addition, lung auscultation revealed weakened or disappeared breath sounds. Patients exhibited other signs of pleural effusion, including chest CT demonstrating pleural effusion and tumor lesions in the lung, and routine examination of pleural fluid was consistent with exudatum according to Light's criteria. Malignant tumors were confirmed by lung biopsy, pleural biopsy or cytologic examination of pleural effusion. Patients with metabolic diseases were excluded, and none of the patients had received chemotherapy, radiotherapy, surgery or other treatment prior to sample collection. All of the malignant tumors were primary.

The L group was formed of transudative pleural effusion (n=18) patients, who were diagnosed following chest pain, dyspnea and other pleural effusion symptoms. Patients exhibited cardiac functional insufficiency, cirrhosis, hypoproteinemia or other basic diseases. Chest physical examination indicated weakened tactile fremitus and percussion dullness in the affected side. Furthermore, lung auscultation revealed weakened or disappeared breath sounds. Patients exhibited other signs of pleural effusion, including pleural effusion as demonstrated by chest CT, although no pulmonary or pleural lesions were observed. The routine examination of pleural fluid was consistent with transudate according to Light's criteria. Pleural effusion was absorbed following improvement of cardiac dysfunction and hypoproteinemia. Patients with metabolic diseases were excluded. The transudative pleural effusion was collected from the subjects prior to the improvement of cardiac dysfunction and hypoproteinemia. Subsequently, screening was performed and samples were selected from patients whose pleural effusion was absorbed following improvement of cardiac dysfunction and hypoproteinemia, to be used in subsequent analyses.

Instruments and reagents. The MHz 600 INOVA superconducting nuclear magnetic resonance spectrometer was purchased from Varian Medical Systems (Palo Alto, CA, USA). It was equipped with a pulsed field gradient, and the gradient field has three resonance probes. The Ependorf MiniSpin Plus centrifuge was obtained from Eppendorf (Hamburg, Germany).

D_2O (concentration, 99.9%) was purchased from Cambridge Isotope Laboratories, Inc. (Tewksbury, MA). The 3-(trimethylsilyl)-propionic acid-D_4 sodium salt (TSP) was purchased from Merck KGaA (Darmstadt, Germany).

Sample preparation. Pleural effusion samples were obtained via thoracentesis. After conventional disinfection, the pleural effusion was collected in sterile test tubes. Each sample (~1 ml) was placed in a refrigerator at -80˚C. Prior to nuclear magnetic resonance (NMR) analysis, the pleural effusion samples were defrosted at room temperature and centrifuged at 4,000 x g, 4˚C for 10 min. Aliquots of 350 μl supernatant were transferred into 5-mm NMR tubes, and mixed with 200 μl D_2O and 50 μl TSP (0.1% w/v in D_2O). D_2O was used for field frequency locking and normal saline was used to maintain normal plasma osmolality.

^{1}H-NMR spectroscopy of pleural effusion samples. ^{1}H-NMR measurements were obtained on a Varian INOVA 600 spectrometer at a ^{1}H frequency of 600.13 MHz. ^{1}H-NMR spectra of the samples were acquired using a solvent pre-saturation pulse sequence to suppress the residual water resonance.

^{1}H-NMR spectra of the samples were acquired using a Carr-Purcell-Meiboom-Gill pulse sequence. Free induction decays (FIDs) were collected at 128-K data points with a spectral width of 8,000 Hz and 32-K sampling points, the cumulative number of 64 times an acquisition time of 2.04 sec, providing a total pulse recycle delay of 2.00 sec. The data were zero filled by a factor, and FIDs were multiplied by an exponential weighting function equivalent to a line broadening of 0.5 Hz prior to the Fourier transform.

Data processing of ^{1}H-NMR spectra. The phase and baseline of all ^{1}H-NMR spectra were manually corrected using Mest Re Nova software (version 9.0.1.13254; Mestrelab Research, Santiago de Compostela, Spain). The range of δ10-0 ppm in standard ^{1}H-NMR spectra was automatically segmented into 400 regions at 0.01-ppm intervals with δ4.4-0.4 ppm. The data from each sample were normalized to total area to correct for the NMR response shift. This divides the spectrum into a specified number of regions and integrates the total signal area within each region to provide a numerical value. These values are then used as variables for data analysis.

Multivariate statistical analysis. The reduced and normalized NMR spectral data were submitted to SIMCA-P version 11.0 (Umetrics; MKS Data Analytics Solutions, Umeå, Sweden) software package for multivariate analysis and to partial least squares discriminant analysis (PLS-DA). SIMCA-P was used to generate all of the PLS-DA models, score plots and was performed to clarify which chemical shift regions carry the separating information. Cross-validation was used to validate the PLS-DA model according to the default settings in the software. Hotelling's T-squared statistic is a generalization of Student's t statistic that is used in multivariate hypothesis testing.

Statistical analysis. SIMCA-P version 11.0 was used for ^{1}H-NMR data analysis. Values were expressed as the mean ± standard deviation (SD). The significantly different expression of compound peaks (variable importance; VIP >1.0) was listed by the software. Subsequently, the differentiated expressions of peaks were analyzed by discriminatory analysis. SPSS version 19.0 statistical software (IBM Corp., Armonk, NY, USA) was used for the statistical analyses of clinical data. Depending on the underlying statistical distribution and the result of the homogeneity test for variance, either one-way analysis of variance (ANOVA) or the Kruskal-Wallis (K-W) test was used. Primary statistical analysis of the pooled data (mean ± SD) was performed with the ANOVA to determine mean differences of metabolites, followed by Student-Newman-Keuls (SNK) test for multiple comparisons. χ^2 test was used to compare categorical variables. $P<0.05$ was considered to indicate a statistically significant difference.

Pathway analysis. In the current study, the different chemical metabolites were performed with MetaboAnalyst (version 2.0; www.metaboanalyst.ca/MetaboAnalyst) web portal for pathway analysis and visualization. In order to obtain more information on the reference of these metabolites, the Kyoto Encyclopedia of Genes and Genomes (KEGG) PATHWAY Database (www.genome.jp/kegg) was searched. Additional powerful pathway enrichment statistical analysis was performed on log-transformed data and Pearson correlations were calculated to evaluate the association between metabolites ($P<0.05$, impact >0.01).

Results

Baseline characteristics. A total of 58 samples were evaluated, 20 of which were from patients with tuberculous pleural effusion (T group), 20 from patients with malignant pleural effusion (C group) and 18 from patients with transudative pleural effusion (L group). The clinical characteristics of the three groups of subjects are summarized in Table I, which also presents the baseline characteristics of the enrolled patients and control subjects. No significant differences in age, sex or body mass index were identified between the three groups ($P>0.05$).

Twenty-six characteristic resonances were observed in pleural effusion of the T, L and C groups (VIP value >1.0), and eight significantly altered metabolites were identified in the pleural effusion. Changes in these metabolites were associated with the glucose, lipid and amino acid metabolism pathways, some of which are involved in alanine, glutamate, methionine, choline, threonine, serine, betaine, lipid, starch, sucrose and pyruvate metabolism, the citrate cycle, glycolysis, gluconeogenesis and phospholipid biosynthesis.

Typical ^{1}H-NMR spectra of pleural effusion samples are presented in (Fig. 1), with the major metabolites in the integrate regions assigned. The spectra were processed and converted into 400 integral regions of 0.01 ppm width. The resonance

Table I. Demographic characteristics of individuals with tuberculous, malignant and transudative pleural effusion.

Variable	Pleural effusion			
	Tuberculous, n=20	Malignant, n=20	Transudative, n=18	P-value
Male (%)	14 (70.00)	16 (80.00)	14 (77.78)	0.741
Age, years	53.20±10.30	55.70±9.90	49.80±15.10	0.317
Body mass index	23.90±2.80	25.10±3.00	23.10±1.90	0.070
Smoking (%)	5 (25.00)	6 (30.00)	4 (22.22)	0.856
Alcohol (%)	3 (15.00)	5 (25.00)	4 (22.22)	0.724
Systolic blood pressure, mmHg	130.10±22.00	128.50±23.00	132.20±22.00	0.878
Diastolic blood pressure, mmHg	69.60±17.20	69.40±10.80	70.20±14.50	0.985

Data are presented as mean ± standard deviation or n (%). Comparison among the groups was conducted using one way analysis of variance for normally distributed variables. χ^2 test was used in categorical variables. There was no significant difference in age, sex, body mass index, smoking, alcohol or blood pressure among these three groups (P>0.05).

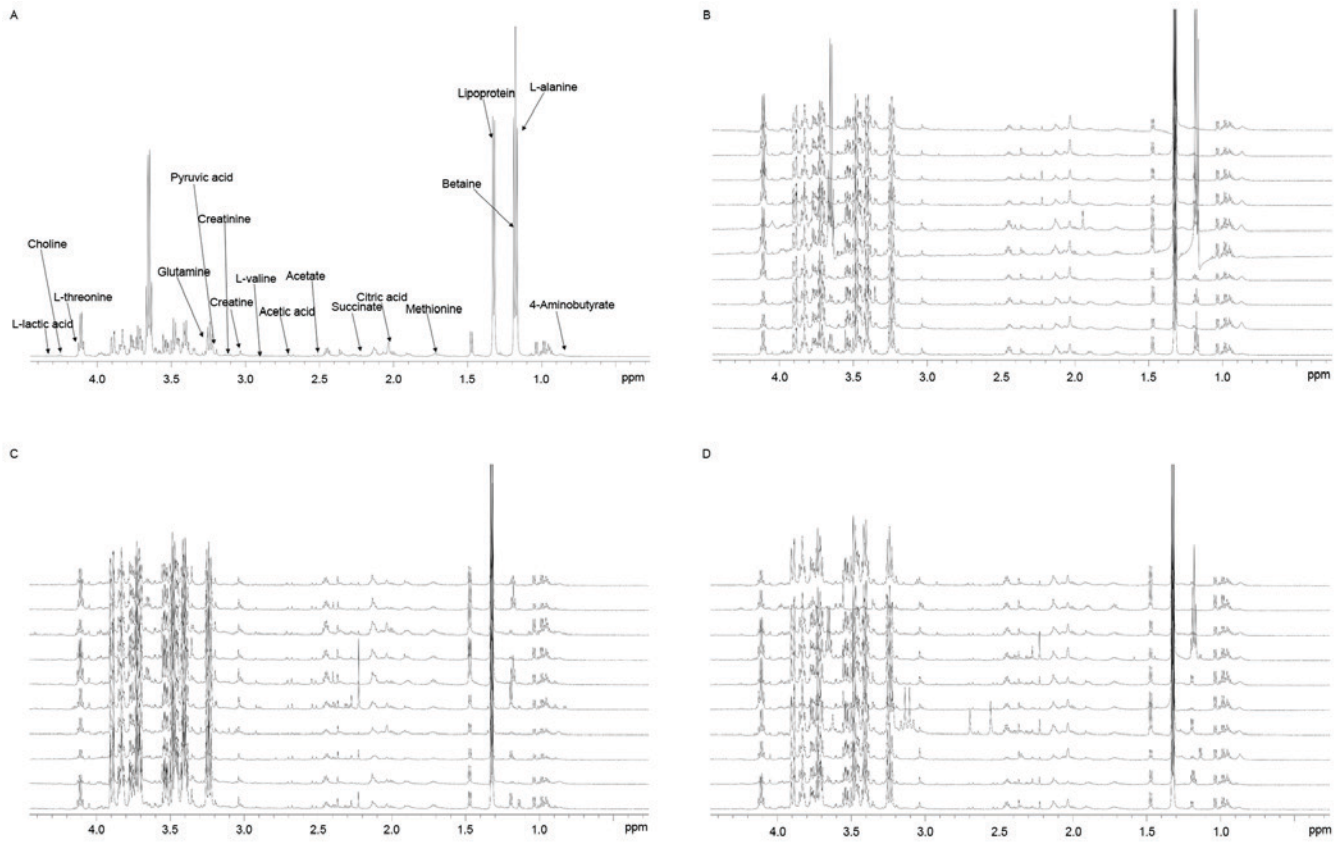

Figure 1. (A) The spectrum displayed a wide range of metabolites, including lipoproteins, organic acids, amino acids and carbohydrates. Typical ^{1}H-nuclear magnetic resonance spectra of pleural effusion samples from the (B) tuberculous, (C) malignant and (D) transudative pleural effusion groups. The spectra were processed and converted into 400 integral regions of 0.01-ppm width.

assignments were made according to published reports and the Metabolomic Toolbox (21,22).

PLS-DA was used to analyze the ^{1}H-NMR metabolite profiles, and the separation was readily detected. The reliability of the established PLS-DA models was evaluated by the explained variation, R^2 and the predicted total variation, Q^2, which is calculated by cross-validation. The expected R^2 and Q^2 depend highly on their application fields, and should be >0.5 and >0.4, respectively, indicating a significant biological model. In our established model for pleural effusion of humans, the value of R^2 was >0.7, indicating that the PLS-DA model had been successfully established (Table II).

The score plots of pleural effusion samples demonstrated good separation in the T and L groups, the T and C groups and the L and C groups. Further analysis of the PLS-DA loading plot indicated that when the variable deviated from the origin,

Table II. Summary of the parameters for assessing the quality of the partial least squares discriminate analysis model.

Model	Principal components obtained by cross-validation, n	R^2X	R^2Y	Q^2
T and L	100	0.226	0.983	0.768
T and C	100	0.182	0.919	0.361
L and C	100	0.283	0.995	0.688

R^2X, variation explanation in X; R^2Y, variation explanation in response to Y; Q^2, predicted variation capability of compound. T, tuberculous pleural effusion group; L, transudative pleural effusion group; C, malignant pleural effusion group.

a higher value of VIP projection was obtained. The differences in metabolite profiling among the three groups were important for biomarker identification for diagnosis and therapy. The analysis demonstrated that the metabolites were modified, and the orthogonal projections to latent structures discriminant analysis (OPLS-DA) model was subsequently used to investigate the metabolites that were differentially regulated. As shown in Fig. 2A, the score plot of principal component (PC) 1 and PC2 indicated that three groups could be clearly separated from each other. The statistical validations of the corresponding OPLS-DA model by permutation analysis are presented in Fig. 2B.

The parameters for different stages were as follows: T and L, R^2=0.79 and Q^2=0.768; T and C, R^2=0.921 and Q^2=0.272; and L and C, R^2=0.963 and Q^2=0.688. When the VIP value was >1.0, the variable was considered as a contributor for the classification of the T and L groups, T and C groups, and L and C groups. The panel of 26 metabolites with VIP >1 of these three groups are presented in Table III.

The pathway analysis was performed by MetaboAnalyst 2.0 (www.metaboanalyst.ca/MetaboAnalyst) with R version 2.15.0 to identify the most relevant pathwa-ys involved in the study conditions. To obtain more information on the reference of these metabolites, the KEGG PATHWAY Database was searched and the altered metabolites were identified to be predominantly involved in amino acid metabolism, glyco-metabolism and lipid metabolism. These metabolic pathways were detected from the above-mentioned differentiating metabolites following performance of a pleural effusion enrichment analysis Fig. 3.

Depending on the result of the homogeneity test for variance and the underlying statistical distribution, ANOVA was used to analyze the parameters of L-alanine, citric acid, betaine, creatine, low-density lipoprotein (LDL), aspartate, pyruvic acid, glutamine, L-glutamine, succinate, acetate, putrescine and L-lactic acid (Table IV). For the ANOVA, a statistically significant difference in the level of L-alanine and citric acid was observed between the three groups (P<0.05). Statistically significant differences in the level of creatine, LDL and L-lactic acid were identified among the three groups (P<0.01). For the SNK tested, the levels of L-alanine, citric acid and creatine were lower in tuberculous pleural effusion when compared

Table III. Identified biomarkers from the three groups.

Compound	^{1}H-nuclear magnetic resonance spectra (ppm)	Variable importance
L-lactic acid	4.28	1.948
Fructose	4.02	1.276
L-Serine	3.96	1.274
Tyrosine	3.95	1.034
L-Alanine	3.76	1.361
L-Threonine	3.59	1.131
Betaine	3.26	1.273
Choline	3.19	1.503
Creatinine	3.10	1.059
Creatine	3.06	1.829
Putrescine	3.04	2.206
Aspartate	2.81	1.169
Methionine	2.64	1.592
Pyruvic acid	2.46	1.170
Glutamine	2.45	1.206
L-glutamine	2.44	1.177
Succinate	2.39	1.569
L-glutamic acid	2.32	1.642
4-Aminobutyrate	2.28	1.532
L-Valine	2.27	1.438
Low-density lipoprotein	1.47	1.135
Citric acid	2.53	1.859
Glutamic acid	2.12	1.125
Acetic acid	1.91	1.478
Acetate	1.90	1.166
Ornithine	1.82	1.329

with in malignant and transudative pleural effusion (P<0.05). The LDL level was lower in the transudative pleural effusion samples when compared with the tuberculous and malignant pleural effusion samples (P<0.05). No significant differences were identified in L-alanine, citric acid and creatine levels between malignant and transudative pleural effusion samples. No significant difference was identified between tuberculous and malignant pleural effusion samples for the LDL level, as well as the level of L-lactic acid between the tuberculous pleural effusion and the transudative pleural effusion samples.

As the parameters did not follow normal distribution, the K-W test was used (Table V). It is hypothesized that these data were significantly influenced by the type of disease and, therefore, did not follow normal distribution. In addition, statistically significant differences were observed in the level of L-threonine and acetic acid between the three groups (P<0.05), and statistically significant differences in the level of methionine were observed between the three groups (P<0.01). A significant increase in the level of acetic acid was observed in malignant pleural effusion patients, as compared with the tuberculous and transudative pleural effusion subjects. No marked difference was noted in the acetic acid level of the tuberculous and

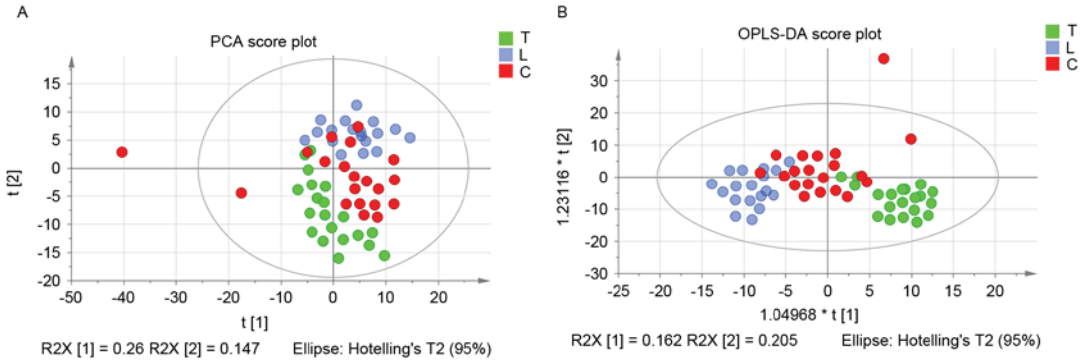

Figure 2. (A) Score plots of pleural effusion samples demonstrated good separation in the tuberculous, transudative and malignant pleural effusion groups. (B) Statistical validation of the corresponding OPLS-DA model by permutation analysis. PCA, principal component analysis; OPLS-DA, orthogonal projections to latent structures discriminant analysis; T, tuberculous pleural effusion group; L, transudative pleural effusion group; C, malignant pleural effusion group.

transudative pleural effusion groups. The levels of methionine were significantly lower in the malignant pleural effusion group when compared with the other groups ($P<0.05$). However, the level of L-threonine was significantly increased in the tuberculous pleural effusion group when compared with transudative pleural effusion groups ($P<0.05$). No obvious difference was observed in the level of L-threonine in the other two groups.

Discussion

Pleural effusion, which has varied causes, is a common clinical manifestation (23). TB remains one of the most frequent causes of pleural effusion, and the pleural form represents 4-10% of all TB cases (24). Malignant pleural effusion represents between 15 and 35% of all pleural effusion cases. Transudative pleural effusion is most often caused by heart failure (80%) (25). Patients rarely receive rapid and accurate diagnosis and treatment. However, with the development and maturation of proteomics, certain markers have been identified, although there is no uniform criteria to guide the diagnosis. Additionally, the diagnostic value of a single marker is limited. In recent years, studies have identified that the metabolic spectrums of active TB, lung cancer and tuberculous meningitis patients are specific (26,27), which provides novel hypotheses for the diagnosis and treatment of this type of disease. In the current study, eight metabolites were identified to be altered significantly in the three groups. In the following discussion, the mechanism underlying the changes in these prominent metabolites, as well as their potential physiological and clinical significance are described.

Pathological changes of citric acid metabolism. Mycobacterium TB is an obligate aerobe, therefore, it is strongly reliant on the tricarboxylic acid (TCA) cycle to obtain energy. Citric acid is an important intermediate product of the TCA cycle, which is catalyzed to isocitric acid by aconitase. Furthermore, mycobacterium TB is reliant on the glyoxylate cycle as a source of metabolites and energy. A functional glyoxylate cycle with its key enzyme, isocitrate lyase is necessary for bacterial survival. Mycobacterium TB in activated macrophages expresses a large quantity of isocitrate lyase, which catalyzes isocitrate into succinate and glyoxylate (28,29). In the present study, the level of citric acid in tuberculous pleural effusion was identified to be significantly lower than in the other groups. The decrease of citric acid in the tuberculous pleural effusion group may be associated with the above-mentioned mechanism. As the utilization of citric acid in mycobacterium TB increased, the level of citric acid was reduced (30).

Citrate synthase, one of the key enzymes in the TCA cycle, catalyzes the reaction between oxaloacetic acid and acetyl coenzyme A (CoA) to generate citrate. Increased citrate synthase has been observed in non-Hodgkin's lymphoma residual disease, pancreatic cancer, colorectal cancer and ovarian carcinoma (31-34). Increasing evidence indicates that citrate synthase activity is closely associated with various types of cancer (32,34). A recent study hypothesized that citrate synthase may contribute to the cancer phenotype, as well as drug resistance and, thus, represent a therapeutic target (34). In this study, the level of citric acid in the malignant pleural effusion group was significantly higher when compared with the mycobacterium tuberculous effusion group. This may be due to the high expression of citrate synthase in tumor tissue. Lipogenesis is essential to cancer cell survival. In the fatty acid synthesis pathway, acetyl-CoA is carboxylated to malonyl-CoA by acetyl-CoA carboxylase. Acetyl-CoA carboxylase, a key enzyme in fatty acid synthesis, and indicates a possible connection between lipid synthesis and genetic factors involved in susceptibility to certain types of cancer (35,36). Citric acid alters the structure of acetyl-CoA carboxylase to activate it from monomers to polymers. This process enhances the catalytic activity of acetyl-CoA carboxylase and creates favorable conditions for the growth of tumor cells, indicating that citric acid is required by tumor cells. The effect of citric acid on acetyl-CoA carboxylase may be associated with the high level of citric acid in the malignant pleural effusion group in the current study.

Pathological changes of lactic acid, creatine and acetic acid metabolism. Tumor cells predominantly produce energy by a high rate of glycolysis followed by lactic acid fermentation in the cytosol. Whereas in the majority of normal cells, a comparatively low rate of glycolysis is followed by oxidation of pyruvate in mitochondria, even under conditions of sufficient oxygen, which is termed the Warburg effect (37).

Table IV. Statistical results of one way analysis of variance and SNK.

Compound	Pleural effusion			F-value	P-value
	Tuberculous, n=20	Malignant, n=20	Transudative, n=18		
L-Alanine	89.51±19.67[a]	108.21±16.04	105.90±16.78	3.369	0.049
Citric acid	19.42±7.20[a]	26.80±6.89	24.26±4.73	4.165	0.027
Betaine	110.51±19.86	130.20±20.40	130.22±28.99	2.351	0.114
Creatine	3.95±1.22[a]	7.67±3.36	7.45±3.21	5.647	0.009
Low-density lipoprotein	37.21±4.00	37.56±12.25	23.11±5.15[a]	10.577	0.000
Aspartate	0.77±0.70	1.56±1.40	1.55±1.19	1.599	0.221
Pyruvic acid	21.88±6.60	25.18±7.86	26.46±9.08	0.893	0.421
Glutamine	37.41±11.96	45.38±11.36	43.90±15.60	1.049	0.364
L-glutamine	38.23±13.00	47.23±12.14	44.75±16.88	1.078	0.354
Succinate	5.34±1.72	7.45±3.86	8.47±2.92	2.895	0.073
Acetate	2.94±0.70	3.26±1.43	3.77±1.08	1.397	0.265
Putrescine	13.81±5.67	14.88±5.11	17.34±5.63	1.094	0.349
L-lactic acid	0.09±0.16	0.68±0.57[a]	0.17±0.24	7.567	0.002

[a]P<0.05 vs. each of the other two groups. Data are presented as mean ± standard deviation.

LDH, a key enzyme that catalyzes the transfer of pyruvate to lactate, is markedly increased in patients with tumors (38). In addition, studies have identified that in addition to glucose, glutamine is significantly consumed by the majority of tumor cells and metabolized to alanine, lactate and ammonium ions (39). The increase of lactic acid and acetic acid in malignant pleural effusion may be associated with the following mechanism: The increased lactic acid, creatine and acetic acid in the tumor tissue causes acidosis, and acidosis promotes the decomposition of the extracellular matrix and the formation of angiogenesis, as well as increasing the proliferation and metastasis of tumor cells (38). Compared with the malignant pleural effusion group, the lactate, creatine and acetic levels of the tuberculous pleural effusion group were lower. This may be due to various reasons. Firstly, mycobacterium TB is an obligate aerobe; therefore, it predominantly produces energy via the TCA cycle. In addition, many *Bacillus*, similar to prokaryotic microorganisms, use glucose, fructose, lactose and organic acids (such as acetic acid, pyruvate and lactate) as their energy and carbon sources.

Pathological changes of lipid metabolism. The lipid of mycobacterium TB accounts for 20-40% of the dry weight of bacteria, and 60% of the dry weight of the cell wall. Mycobacterium TB and other mycobacteria have a distinct cell wall, which has a lipid-rich outer layer. Acylated trehaloses, trehalose dimycolate and trehalose monomycolate (well characterized mycobacterium TB virulence factors) are abundant in the mycobacterial cell wall (40). Mycolic acids are vital components of mycobacterium TB. The biosynthesis of mycolic acids is linked to the activity of fatty acid synthases (41). Cholesterol is an important nutrient for mycobacterium TB. The catabolism of cholesterol has multiple functions during macrophage infection; it is used to supply carbon to the central metabolism of mycobacterium TB as succinate and pyruvate. It is also involved in the modulation of intracellular trafficking and immune signaling (42,43). Peroxisome proliferator-activated receptor γ (PPARγ) is a member of the lipid-activated nuclear receptor family and has been demonstrated to function as a key transcriptional regulator of lipid metabolism in macrophages, dendritic cells, and T and B cells (44). The PPARγ transcription factor directly regulates the expression of various genes participating in fatty acid uptake, lipid storage, and inflammatory response. Previous studies demonstrated that the mycobacterium infection induces the expression and activation of PPARγ (45).

In the current study, the lipid levels in tuberculous pleural effusion samples were significantly higher than in the transudative pleural effusion samples, which may be associated with the large number of lipids in TB bacteria. However, compared with malignant pleural effusion, the lipid levels in tuberculous pleural effusion were not significantly different. This may be associated with the lipid content in tumors; it has been identified that the content of lipid increases in the majority of tumors (46). The present study indicates that the pleural effusion of patients with pulmonary TB demonstrates lipid metabolism disorders. The present microbiology studies demonstrated that the fatty acid composition in the bacterial cell structure is highly homologous to the DNA of the bacteria. The characteristics of fatty acids, such as type and quantity, provide the basis for the identification of mycobacterium species (47).

Pathological changes of amino acid metabolism. Oxygen saturation decreases and the energy consumed by the maintenance of breathing increases in patients with severe pulmonary TB and pulmonary dysfunction. When the energy intake is insufficient, mytolin is decomposed into amino acids, such as threonine, that are used for gluconeogenesis. In the current study, the increase of threonine in tuberculous pleural effusion

Table V. Statistical results of Kruskal-Wallis test.

Compound	Pleural effusion				
	Tuberculous, n=20	Malignant, n=20	Transudative, n=18	χ^2	P-value
Fructose	11.65	17.95	16.90	4.175	0.124
L-Serine	13.80	18.60	14.10	1.866	0.393
Tyrosine	15.10	16.90	14.50	0.403	0.818
L-Threonine	20.90[a]	14.90	10.70	6.782	0.034
Creatinine	18.20	10.00	18.30	5.855	0.054
Choline	20.80	11.40	14.30	5.979	0.050
Methionine	17.00	8.80[a]	20.70	9.572	0.008
Acetic acid	13.60	18.20[b]	14.70	7.760	0.020
L-Valine	20.10	13.00	13.40	4.106	0.128
Glutamic acid	16.00	13.50	17.00	0.839	0.657
4-Aminobutyrate	20.80	11.40	14.30	2.147	0.342
L-glutamic acid	19.30	11.30	15.90	4.160	0.125
Ornthine	15.80	12.10	17.30	2.240	0.326

[a]P<0.05 vs. transudative pleural effusion. [b]P<0.05 vs. each of the other two groups. Data are presented as the mean rank.

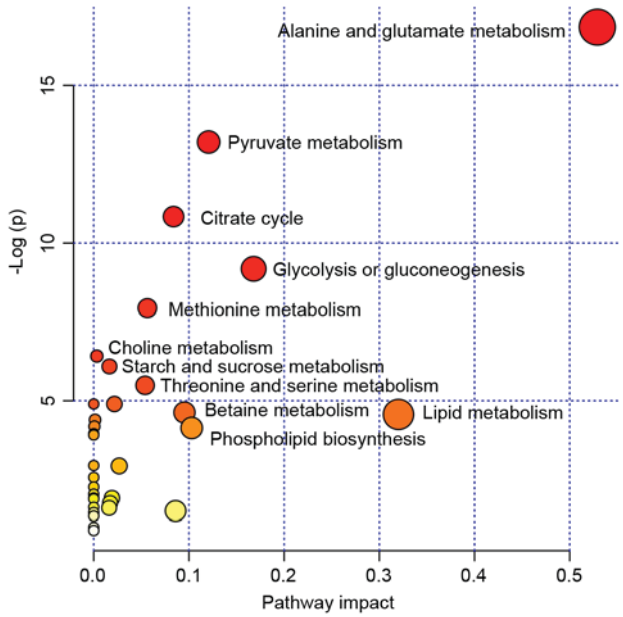

Figure 3. MSEA was implemented to evaluate metabolic pathway enrichment among the tuberculous, transudative and malignant pleural effusion groups. MSEA indicated that the alanine, glutamate, methionine, choline, threonine, serine, betaine, lipid, starch, sucrose and pyruvate metabolism, and citrate cycle, glycolysis, gluconeogenesis and phospholipid biosynthesis are significantly associated with these diseases. MSEA, metabolite set enrichment analysis.

may be released from other tissue in order to meet the requirement of *tubercle bacillus*. Threonine is an essential amino acid, which is involved in the composition of the immune system. As patients suffer from inflammation, the demand for threonine increases, which has an anti-oxidative effect. Furthermore, the activation of T cells requires different types of amino acid. The mycobacterium TB genome has a number of genes, which encode proteins associated with antigen variation and immune evasion. Different types of bacteria use different amino acids as sources of nitrogen, carbon and energy. In the tuberculous pleural effusion group, the level of threonine significantly increased, indicating an amino acid metabolism disorder which may block threonine metabolism. The increased threonine may additionally be produced by mycobacterium TB. The specific mechanism requires further investigation. Establishing the amino acid status of TB patients provides the basis for differential diagnosis, facilitates nutritional support therapy and enhances the immune system of patients.

Patients with cancer are characterized by increased energy consumption, negative nitrogen balance, increased glutamine utilization and amino acid metabolism disorders. In the malignant transformation of tumor tissues, the dynamic changes in tumor cells lead to the occurrence of amino acid metabolic defects. It was found that the tumor cells selectively absorb certain amino acids in the plasma, which meet their growth requirement, and leads to the disordered amino acid metabolism. Tumors utilize branched chain amino acids for protein synthesis and may oxidize them either partially or completely. Weight loss and malnutrition are among the most common features observed in cancer patients experiencing prolonged catabolic stress. Numerous studies focus on the concept of imbalanced amino acid therapy, which alters the proportion of certain amino acid supplies, resulting in synthesis and metabolism disorders of proteins in tumors and typically favors the host (48,49). Furthermore, many studies aim to establish anti-tumor drugs that are more efficient and less toxic. In a previous study, amino acids, which are required by malignant tumor cells, were included in the anti-tumor medicine to increase the efficacy of these medicines (50). In the present study, decreased methionine in malignant pleural effusion samples may have been associated with the increased oxidation of amino acids, which is a metabolic response that compensates for the increased energy

expenditure and glutamine consumption. In addition, treatments (particularly chemotherapy treatments) may alter amino acid supply and demand (48). Furthermore, disordered amino acid metabolism may depend on specific tumor type and physiological characteristics, including synthetic rate, volume of tumor, and rate of proliferation (48). The potential role of amino acid metabolism in malignant pleural effusion remains unclear, thus, the specific mechanism requires further investigation.

In conclusion, ^{1}H-NMR-based metabolomic analysis provides a platform for the identification of small molecule metabolite spectrums and biomarker metabolites, as well as associated pathophysiologic and molecular biological pathways in TB, malignant and transudative pleural effusion. The current results indicated the ^{1}H-NMR-based metabolite profiling is promising for differentiating TB, malignant and transudative pleural effusion, which exhibit morphological similarity. The findings provide novel insights into the underlying mechanisms of these diseases, and may offer further avenues for diagnosis and therapeutic strategies.

Acknowledgements

The authors would like to thank the clinical staff of the Second Department of Respiratory Medicine in the First Affiliated Hospital of Kunming Medical University (Kunming, China), for their care of the study subjects and support with pleural effusion sample collection. The authors are grateful to Dr Yan Li and the staff at Fan-Xing Biological Technology Research Laboratory (Beijing, China) for their assistance with the experiment.

References

1. Maskell N; British Thoracic Society Pleural Disease Guideline Group: British thoracic society pleural disease guidelines-2010 update. Thorax 65: 667-669, 2010.
2. Light RW: Clinical practice: Pleural effusion. N Engl J Med 346: 1971-1977, 2002.
3. Daniil ZD, Zintzaras E, Kiropoulos T, Papaioannou AI, Koutsokera A, Kastanis A and Gourgoulianis KI: Discrimination of exudative pleural effusions based on multiple biological parameters. Eur Respir J 30: 957-964, 2007.
4. World Health Organization: Global Tuberculosis report, Geneva, Switzerland, 2015.
5. Light RW: Update on tuberculous pleural effusion. Respirology 15: 451-458, 2010.
6. Dodd PJ, Gardiner E, Coghlan R and Seddon JA: Burden of childhood tuberculosis in 22 high-burden countries: A mathematical modelling study. Lancet Glob Health 2: e453-e459, 2014.
7. Nicholson JK, Lindon JC and Holmes E: 'Metabonomics': Understanding the metabolic responses of living systems to pathophysiological stimuli via multivariate statistical analysis of biological NMR spectroscopic data. Xenobiotica 29: 1181-1189, 1999.
8. Schmidt CW: Metabolomics: What's happening downstream of DNA. Environ Health Perspect 112: A410-A415, 2004.
9. Illig T, Gieger C, Zhai G, Römisch-Margl W, Wang-Sattler R, Prehn C, Altmaier E, Kastenmüller G, Kato BS, Mewes HW, *et al*: A genome-wide perspective of genetic variation inhuman metabolism. Nat Genet 42: 137-141, 2010.
10. Yang J, Xu G, Zheng Y, Kong H, Pang T, Lv S and Yang Q: Diagnosis of liver cancer using HPLC-based metabonomics avoiding false-positive result from hepatitis and hepatocirrhosis diseases. J Chromatogr B Analyt Technol Biomed Life Sci 813: 59-65, 2004.
11. Chen J, Zhang X, Cao R, Lu X, Zhao S, Fekete A, Huang Q, Schmitt-Kopplin P, Wang Y, Xu Z, *et al*: Serum 27-nor-5β-cholestane-3,7,12,24,25 pentol glucuronide discovered by metabolomics as potential diagnostic biomarker for epithelium ovarian cancer. J Proteome Res 10: 2625-2632, 2011.
12. Hodavance MS, Ralston SL and Pelczer I: Beyond blood sugar: The potential of NMR-based metabonomics for type 2 human diabetes, and the horse as a possible model. Anal Bioanal Chem 387: 533-537, 2007.
13. Mäkinen VP, Soininen P, Forsblom C, Parkkonen M, Ingman P, Kaski K, Groop PH and Ala-Korpela M; FinnDiane Study Group: Diagnosing diabetic nephropathy by 1H NMR metabonomics of serum. Magma 19: 281-296, 2006.
14. Messana I, Forni F, Ferrari F, Rossi C, Giardina B and Zuppi C: Proton nuclear magnetic resonance spectral profiles of urine in type II diabetic patients. Clin Chem 44: 1529-1534, 1998.
15. Brindle JT, Nicholson JK, Schofield PM, Grainger DJ and Holmes E: Application of chemometrics to 1H NMR spectroscopic data to investigate a relationship between human serum metabolic profiles and hypertension. Analyst 128: 32-36, 2003.
16. Brindle JT, Antti H, Holmes E, Tranter G, Nicholson JK, Bethell HW, Clarke S, Schofield PM, McKilligin E, Mosedale DE and Grainger DJ: Rapid and noninvasive diagnosis of the presence and severity of coronary heart disease using 1H-NMR-based metabonomics. Nat Med 8: 1439-1444, 2002.
17. Sabatine MS, Liu E, Morrow DA, Heller E, Mc Carroll R, Wiegand R, Berriz GF, Roth FP and Gerszten RE: Metabolonmic identification of novel biomarkers of myocardial ischemia. Circulation 112: 3868-3875, 2005.
18. Barba I, de León G, Martín E, Cuevas A, Aguade S, Candell-Riera J, Barrabés JA and Garcia-Dorado D: Nuclear magnetic resonance-based metabolomics predicts exercise-induced ischemia in patients with suspected coronary artery disease. Magn Reson Med 60: 27-32, 2008.
19. Sun L, Hu W, Liu Q, Hao Q, Sun B, Zhang Q, Mao S, Qiao J and Yan X: Metabonomics reveals plasma metabolic changes and inflammatory marker in polycystic ovary syndrome patients. J Proteome Res 11: 2937-2946, 2012.
20. Zheng P, Gao HC, Li Q, Shao WH, Zhang ML, Cheng K, Yang DY, Fan SH, Chen L, Fang L and Xie P: Plasma metabonomics as novel diagnostic approach for major depressive disorder. J Proteome Res 11: 1741-1748, 2012.
21. Xia J, Mandal R, Sinelnikov IV, Broadhurst D and Wishart DS: MetaboAnalyst 2.0-a comprehensive server for metabolomic data analysis. Nucleic Acids Res 40: W127-W133, 2012.
22. Xia J and Wishart DS: Metabolomic data processing, analysis, and interpretation using MetaboAnalyst. Curr Protoc Bioinformatics Chapter 14: Unit 14.10, 2011.
23. Yang WB, Liang QL, Ye ZJ, Niu CM, Ma WL, Xiong XZ, Du RH, Zhou Q, Zhang JC and Shi HZ: Cell origins and diagnostic accuracy of interleukin 27 in pleural effusions. PLoS One 7: e40450, 2012.
24. Dong X and Yang J: High IL-35 pleural expression in patients with tuberculous pleural effusion. Med Sci Monit 21: 1261-1268, 2015.
25. Villena Garrido V, Cases Viedma E, Fernández Villar A, de Pablo Gafas A, Pérez Rodríguez E, Porcel Pérez JM, Rodríguez Panadero F, Ruiz Martínez C, Salvatierra Velázquez A and Valdés Cuadrado L: Recommendations of diagnosis and treatment of pleural effusion. Update. Arch Bronconeumol 50: 235-249, 2014 (In English, Spanish).
26. Frediani JK, Jones DP, Tukvadze N, Uppal K, Sanikidze E, Kipiani M, Tran VT, Hebbar G, Walker DI, Kempker RR, *et al*: Plasma metabolomics in human pulmonary tuberculosis disease: A pilot study. PLoS One 9: e108854, 2014.
27. Deja S, Porebska I, Kowal A, Zabek A, Barg W, Pawelczyk K, Stanimirova I, Daszykowski M, Korzeniewska A, Jankowska R and Mlynarz P: Metabolomics provide new insights on lung cancer staging and discrimination from chronic obstructive pulmonary disease. J Pharm Biomed Anal 100: 369-380, 2014.
28. Nandakumar M, Nathan C and Rhee KY: Isocitrate lyase mediates broad antibiotic tolerance in *Mycobacterium tuberculosis*. Nat Commun 5: 4306, 2014.
29. Eoh H and Rhee KY: Multifunctional essentiality of succinate metabolism in adaptation to hypoxia in Mycobacterium tuberculosis. Proc Natl Acad Sci USA 110: 6554-6559, 2013.
30. Micklinghoff JC, Breitinger KJ, Schmidt M, Geffers R, Eikmanns BJ and Bange FC: Role of the transcriptional regulator RamB (Rv0465c) in the control of the glyoxylate cycle in *Mycobacterium tuberculosis*. J Bacteriol 191: 7260-7269, 2009.
31. Kusao I, Troelstrup D and Shiramizu B: Possible mitochondria-associated enzymatic role in Non-Hodgkin lymphoma residual disease. Cancer Growth Metastasis 1: 3-8, 2008.
32. Schlichtholz B, Turyn J, Goyke E, Biernacki M, Jaskiewicz K, Sledzinski Z and Swierczynski J: Enhanced citrate synthase activity in human pancreatic cancer. Pancreas 30: 99-104, 2005.

33. Qiu Y, Cai G, Su M, Chen T, Liu Y, Xu Y, Ni Y, Zhao A, Cai S, Xu LX and Jia W: Urinary metabonomic study on colorectal cancer. J Proteome Res Mar 9: 1627-1634, 2010.
34. Chen L, Liu T, Zhou J, Wang Y, Wang X, Di W and Zhang S: Citrate synthase expression affects tumor phenotype and drug resistance in human ovarian carcinoma. PLoS One 9: e115708, 2014.
35. Chajès V, Cambot M, Moreau K, Lenoir GM and Joulin V: Acetyl-CoA carboxylase alpha is essential to breast cancer cell survival. Cancer Res 66: 5287-5294, 2006.
36. Brusselmans K, De Schrijver E, Verhoeven G and Swinnen JV: RNA interference-mediated silencing of the acetyl-CoA-carboxylase-α gene induces growth inhibition and apoptosis of prostate cancer cells. Cancer Res 65: 6719-6725, 2005.
37. Warburg O: On the origin of cancer cells. Science 123: 309-314, 1956.
38. Kayser G, Kassem A, Sienel W, Schulte-Uentrop L, Mattern D, Aumann K, Stickeler E, Werner M, Passlick B and zur Hausen A: Lactate-dehydrogenase 5 is overexpressed in non-small cell lung cancer and correlates with the expression of the transketolase-like protein 1. Diagn Pathol 5: 22, 2010.
39. Chen JQ and Russo J: Dysregulation of glucose transport, glycolysis, TCA cycle and glutaminolysis by oncogenes and tumor suppressors in cancer cells. Biochim Biophys Acta 1826: 370-384, 2012.
40. Gilmore SA, Schelle MW, Holsclaw CM, Leigh CD, Jain M, Cox JS, Leary JA and Bertozzi CR: Sulfolipid-1 biosynthesis restricts *Mycobacterium tuberculosis* growth in human macrophages. ACS Chem Biol 7: 863-870, 2012.
41. Brown AK, Bhatt A, Singh A, Saparia E, Evans AF and Besra GS: Identification of the dehydratase component of the mycobacterial mycolic acid-synthesizing fatty acid synthase-II complex. Microbiology 153: 4166-4173, 2007.
42. Klink M, Brzezinska M, Szulc I, Brzostek A, Kielbik M, Sulowska Z and Dziadek J: Cholesterol oxidase is indispensable in the pathogenesis of *Mycobacterium tuberculosis*. PLoS One 8: e73333, 2013.
43. Ouellet H, Johnston JB and de Montellano PR: Cholesterol catabolism as a therapeutic target in *Mycobacterium tuberculosis*. Trends Microbiol 19: 530-539, 2011.
44. Szatmari I and Nagy L: Nuclear receptor signalling in dendritic cells connects lipids, the genome and immune function. EMBO J 27: 2353-2362, 2008.
45. Almeida PE, Silva AR, Maya-Monteiro CM, Töröcsik D, D'Avila H, Dezsö B, Magalhães KG, Castro-Faria-Neto HC, Nagy L and Bozza PT: *Mycobacterium bovis* bacillus Calmette-Guérin infection induces TLR2-dependent peroxisome proliferator-activated receptor gamma expression and activation: Functions in inflammation, lipid metabolism, and pathogenesis. J Immunol 183: 1337-1345, 2009.
46. Chen W, Zu Y, Huang Q, Chen F, Wang G, Lan W, Bai C, Lu S, Yue Y and Deng F: Study on metabonomic characteristics of human lung cancer using high resolution magic-angle spinning 1H NMR spectroscopy and multivariate data analysis. Magn Reson Med 66: 1531-1540, 2011.
47. Collins MD, Goodfellow M and Minnikin DE: Fatty acid composition of some mycolic acid-containing coryneform bacteria. J Gen Microbiol 128: 2503-2509, 1982.
48. Baracos VE and Mackenzie ML: Investigations of branched-chain amino acids and their metabolites in animal models of cancer. J Nutr 136 (Suppl 1): S237-S242, 2006.
49. Choudry HA, Pan M, Karinch AM and Souba WW: Branched-chain amino acid-enriched nutritional support in surgical and cancer patients. J Nutr 136 (Suppl 1): S314-S318, 2006.
50. Liu B, Cui C, Duan W, Zhao M, Peng S, Wang L, Liu H and Cui G: Synthesis and evaluation of anti-tumor activities of N4 fatty acyl amino acid derivatives of 1-beta-arabinofuranosylcytosine. Eur Med Chem 44: 3596-3600, 2009.